Forschung im Ingenieurwesen (2025)89:10
https://doi.org/10.1007/s10010-025-00797-z

ORIGINALARBEITEN/ORIGINALS

Investigation into the design of a novel conical plain bearing concept with enhanced serviceability

Jan Euler[1] · Georg Jacobs[1] · Urs Zweiffel[1] · Timm Jakobs[1] · Thomas Decker[1] · Julian Röder[1]

Received: 16 September 2024 / Accepted: 30 January 2025
© The Author(s) 2025

Abstract

Wind power constitutes a significant share in the German energy mix, and future increase is forecast. About 20% of the levelized cost of electricity for wind power stem from maintenance and repair efforts. Wind turbine main bearings are a component especially prone to failure with a failure probability of up to 30% over the wind turbine design lifetime. The current commercially available generation of wind turbines exclusively use rolling element bearings as main bearings. Their exchange or repair is very elaborate as they require a dismantling of the rotor.

At present there are efforts within industry and science to explore plain bearings as a possible alternative to rolling element bearings as wind turbine main bearings. Segmented plain bearings promise reduced repair costs as their segments can be exchanged individually in case of damage or failure without dismantling of the rotor. Three such plain bearing concepts (HydroLa, FlexPad and Z-Pad) were developed. FlexPad features stationary sliding segments with a flexible support structure. The FlexPad however, demonstrated challenges for upscaling towards multi-megawatt turbines regarding e.g. its maintenance. To address the maintenance challenge, the Z-Pad was developed. Z-Pad features its sliding segments on the rotating shaft. Thus, allowing for easier access of the sliding segments. As with the FlexPad bearing no standardised design process exists. However, a process can be developed analogues to the FlexPad design approach. The proposed design process follows the following steps parameter space definition, sampling, elasto-hydrodynamic simulations, surrogate model creation and lastly mathematical optimisation. This study aims to evaluate the underlying parameter set for the future design process. Results from a systematic sensitivity analysis are explored, highlighting the design influence of individual parameters. The study shows, that during design the global design parameters can no longer be considered concurrently with the parameters governing the bearings flexibility. Moreover, unnecessary design features are identified and removed.

Untersuchung des Designs eines neuartigen konischen Gleitlagerkonzepts mit verbesserter Wartungsfreundlichkeit

Zusammenfassung

Windenergie stellt einen bedeutenden Anteil im deutschen Energiemix dar, und ein zukünftiger Anstieg wird prognostiziert. Etwa 20 % der Stromgestehungskosten für Windenergie entfallen auf Wartungs- und Reparaturaufwand. Hauptlager von Windturbinen sind besonders ausfallgefährdete Komponenten mit einer Ausfallwahrscheinlichkeit von bis zu 30 % über die Auslegungslebensdauer der Windturbine. Die derzeit kommerziell verfügbare Generation von Windturbinen verwendet ausschließlich Wälzlager als Hauptlager. Deren Austausch oder Reparatur ist sehr aufwendig, da sie eine Demontage des Rotors erfordern.

✉ Jan Euler
Jan.euler@cwd.rwth-aachen.de

[1] Chair for Wind Power Drives, RWTH Aachen University, Campus-Boulevard 61, 52074 Aachen, Germany

Published online: 11 February 2025

Derzeit gibt es Bemühungen in Industrie und Wissenschaft, Gleitlager als mögliche Alternative zu Wälzlagern als Hauptlager von Windturbinen zu erforschen. Segmentierte Gleitlager versprechen reduzierte Reparaturkosten, da ihre Segmente im Falle von Schäden oder Ausfällen einzeln ohne Demontage des Rotors ausgetauscht werden können. Am CWD wurden drei solche Gleitlagerkonzepte (HydroLa, FlexPad und Z-Pad) entwickelt. Das FlexPad verfügt über stationäre Gleitsegmente mit einer flexiblen Stützstruktur. Das FlexPad zeigte jedoch Herausforderungen bei der Skalierung auf Multi-Megawatt-Turbinen, insbesondere hinsichtlich der Wartung. Um dieses Wartungsproblem anzugehen, wurde das Z-Pad entwickelt. Beim Z-Pad sind die Gleitsegmente auf der rotierenden Welle platziert, was einen einfacheren Zugang zu den Gleitsegmenten ermöglicht. Wie beim FlexPad-Lager existiert kein standardisierter Konstruktionsprozess. Es kann jedoch ein Prozess analog zum FlexPad-Konstruktionsansatz entwickelt werden. Der vorgeschlagene Konstruktionsprozess umfasst die folgenden Schritte: Definition des Parameterraums, Stichprobenziehung der Parameter, elasto-hydrodynamische Simulationen, Erstellung eines Surrogatmodells und schließlich mathematische Optimierung. Diese Studie zielt darauf ab, den zugrunde liegenden Parametersatz für den zukünftigen Konstruktionsprozess zu evaluieren. Ergebnisse aus einer systematischen Sensitivitätsanalyse werden untersucht, wobei der Einfluss einzelner Parameter auf das Design hervorgehoben wird. Die Studie zeigt, dass während des Designs die globalen Designelemente nicht mehr gleichzeitig mit den Parametern berücksichtigt werden können, die die Flexibilität der Lager steuern. Darüber hinaus werden unnötige Konstruktionsmerkmale identifiziert und entfernt.

1 Introduction

Electricity from wind turbines plays a crucial role in the European power supply with ambitious expansion targets for the near future [1–4]. As for every electricity source the levelised cost of electricity (LCOE) is an important metric for wind power, in European markets. Component failure increases the LCOE due to significant maintenance expenditures and yield loss during wind turbine (WT) downtime significantly [5–7]. Main bearings are an important wind turbine component, which still suffer from failures ahead of the designated life [8]. At the time of writing, rolling element bearings are exclusively used for commercially available WT main bearings. The exchange of a failed rolling element main bearing is especially elaborate as the turbine's rotor needs to be dismounted. Using segmented plain bearings as rotor main bearings, downtime and repair cost can potentially be reduced since the segmented nature of the bearings allows for a segment wise exchange or repair of faulty main bearings. Currently there is a variety of concepts for plain bearings as WT main bearings in industrial and scientific research. Three such concepts were subject of public research. First, there was the HydroLa bearing concept as a combination of axial and radial plain bearings. Second, the double flexible conical FlexPad concept. Both the HydroLa and the FlexPad were constructed and tested on a test bench. Lastly, there is the Z-Pad concept, which is described in more detail below since it is the main focus of this paper. The FlexPad and the Z-Pad both function as moment bearings and feature a conical sliding surface design [9–13]. The Z-Pad was specifically designed to tackle the limited serviceability and high run-out of the FlexPad for large scale WTs [12, 14]. The Z-Pad (see Fig. 1) does so by featuring its segments on the rotating shaft rather than on the stationary housing, thus allowing the segments to be rotated into a suitable maintenance position. The Z-Pad concept is also inherently stiffer than the previously developed FlexPad, thus reducing run-out. The design details were presented in [12]. The overall function of the design is analogous to the FlexPad described in [11, 15].

In the course of the FlexPad project a design process for conical plain bearings was proposed [9, 10]. The proposed design process is based on the mathematical optimization of specific target values using surrogate models. The founda-

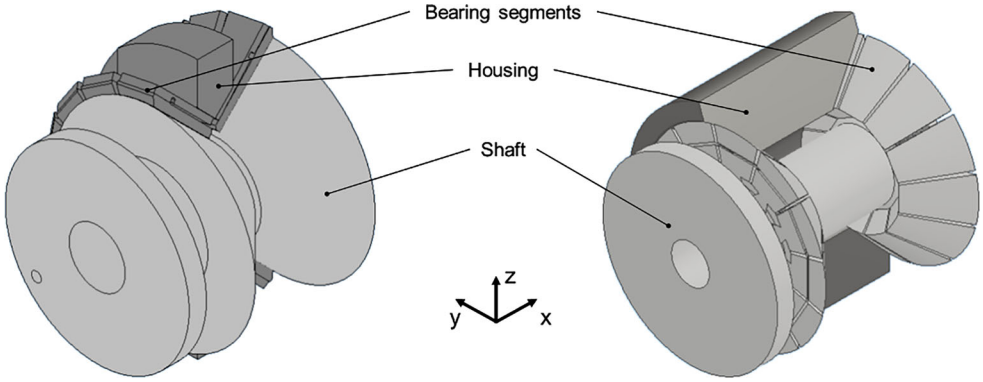

Fig. 1 Concept sketches of the FlexPad bearing (left) and the Z-Pad bearing (right)

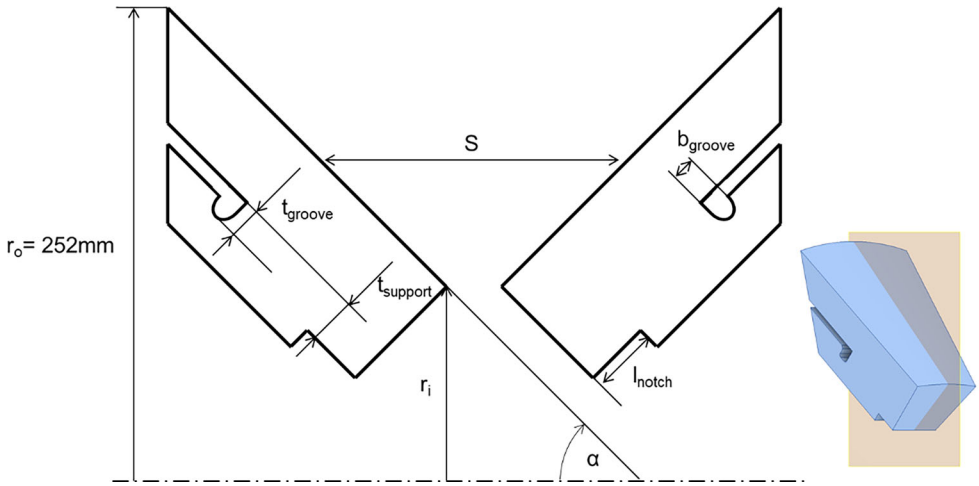

Fig. 2 Z-Pad segment with relevant design parameters

tion for the surrogate models is given via multi-body elasto-hydrodynamic (MB-EHD) simulation results for numerous bearing designs, varied in their key design parameters. In order to create a meaningful basis for the following design process. A clear understanding about the significant parameters and their potential influence is therefore essential. The FlexPads respective design approach is especially tailored for the FlexPad. The Z-Pad shares design features with the Z-Pad due to their mutual conical shape. The flexibility of the Z-Pad however, is governed by a wholly different set of parameters then the FlexPad. A transfer to the Z-Pad is not possible without adaptation. To this end a study analogous to Rolink et al. [16] needs to be performed for the Z-Pad design. This study therefore investigates the influence of individual design parameters of the Z-Pad on its overall performance during constant production load conditions.

2 Methods

As with the FlexPad the hydrodynamic performance of the Z-Pad is governed by the shape and size of the bearing cones as well as by the flexibility of the segments and their support structure. The relevant parameters are depicted in Fig. 2. Compared to common axial or radial plain bearings the geometry is visibly more complex.

Due to the geometric complexity of the Z-Pad a deeper understanding of the individual parameters and their influence of the bearing's performance is necessary. The aim of this study is a higher understanding of the individual design features, via a simulative parameter screening to determine the most relevant parameters for future design. Rolink et al. performed an investigation on the geometry parameters of the FlexPad concept in [16]. In this former study a Plackett-Burman test field was designed and carried out via simulations for the FlexPad. This was also done to achieve a higher understanding of the influence of individual design features. To maintain as much comparability between this work and the FlexPad investigations the selected parameters for the Z-Pad are analogous to parameters chosen in [16]. The Z-Pad and the FlexPad discussed in [16] therefore have the same global design parameter scale (e.g. diameter, width, etc.). Similar to [16] a two level Plackett-Burman test field is used here. Plackett-Burman test fields allow for an assessment of a parameter's general influence on bearing performance while keeping necessary computation and model creation time minimal [17]. The derived test field is shown in Table 1. Twelve different bearing designs were investigated. The bearing geometry is defined by the individual parameter sets P1–P12. For each parameter two numerical values were chosen. The numerically lower parameter values are **highlighted bold** and the higher numerical values are *highlighted italic*. As far as possible the numerical value of the parameter sets for the test field were chosen so that the numerical difference between the red and green values is identical as in [16]. If this was not possible, the parameter span width was adjusted according to the available design space.

For the Parameter sets P1–P12 MB-EHD simulations were performed using the software IST FIRST. The simulation setup was identical to the one used in [12] with the overall model configuration corresponding to the simulation model developed during the FlexPad project by the IST [18]. The same stationary production load conditions were investigated as in ([10, 12, 16, 19–22]; see; Table 2). The selected output values are the maximum total pressure, the total amount of friction loss, the position of maximum pressure, the percentage of area loaded with pressure higher than 1 Pa and the main shaft run-out. Friction loss and main shaft run-out were added as the Z-Pad could demonstrate superior behavior compared to the FlexPad regarding these outputs and they therefore warrant further observation [12].

Table 1 Plackett-Burman test field for parameter screening of the Z-Pad bearing

	α [°]	R_o [mm]	R_i [mm]	S [mm]	n [–]	Ψ [‰]	T_{groove} [mm]	B_{groove} [mm]	$T_{support}$ [mm]	L_{notch} [mm]
P1	**48**	**252**	**133**	**325**	**14**	**0.5**	**11.2**	**13.1**	**18.5**	**27**
P2	*42*	**252**	*108*	325	**14**	0.5	*7.2*	*3.1*	**18.5**	*7*
P3	*42*	*227*	**133**	*275*	**14**	*0.3*	**11.2**	*3.1*	**18.5**	**27**
P4	**48**	*227*	*108*	**325**	*12*	*0.3*	**11.2**	**13.1**	**18.5**	*7*
P5	*42*	252	*108*	*275*	**14**	*0.3*	**11.2**	**13.1**	*14.5*	*7*
P6	*42*	*227*	**133**	*275*	*12*	**0.5**	*7.2*	**13.1**	**18.5**	*7*
P7	*42*	*227*	*108*	**325**	*12*	**0.5**	**11.2**	*3.1*	*14.5*	**27**
P8	**48**	*227*	*108*	*275*	**14**	**0.5**	*7.2*	**13.1**	*14.5*	**27**
P9	**48**	**252**	*108*	*275*	*12*	*0.3*	*7.2*	*3.1*	**18.5**	**27**
P10	**48**	**252**	**133**	*275*	*12*	**0.5**	**11.2**	*3.1*	*14.5*	*7*
P11	*42*	**252**	**133**	**325**	*12*	*0.3*	*7.2*	**13.1**	*14.5*	**27**
P12	**48**	*227*	**133**	**325**	**14**	*0.3*	*7.2*	*3.1*	*14.5*	*7*

Table 2 Load conditions under investigation

Fx [kN]	Fy [kN]	Fz [kN]	My [kN]	Mz [kN]
29.22	2.62	–26.0	22.11	21.32

3 Results and discussion

In the following chapter the simulation results for the effects of the individual design parameters on the bearing's performance are shown. In Fig. 3, 4, 5, 6 and 7 the effect of each individual parameter is shown for the respective output value. Red markings denote the mean output value for designs using the lower parameter value, while the green markings denote the mean output value for simulations for designs using the higher parameter value (color coding as in Table 1). The dotted line denotes the overall average. The parameters are investigated on their relative significance regarding the respective output value.

3.1 Parameter effect regarding maximum total pressure

The results regarding maximum total pressure are shown in Fig. 3. All parameters but width of the groove b_{groove} show significant influence on the maximum pressure. The effect is greatest for the increase of the inner radius r_i where an increase leads to a severe reduction of maximum pressure. The cone angle α, the number of segments N and the clearance ψ are of medium influence. A higher cone angle α results in a decreased maximum pressure, while more segments N and higher amounts of clearance ψ increase maximum pressure. The effect of the remaining parameters is comparatively small.

The effect of the inner radius r_i is opposite to the observation for the FlexPad in [16], where an increase in sliding surface area generally resulted in a reduction of maximum pressure. The inner and outer edge of each segment can bend under pressure to prevent edgewear, which is a fun-

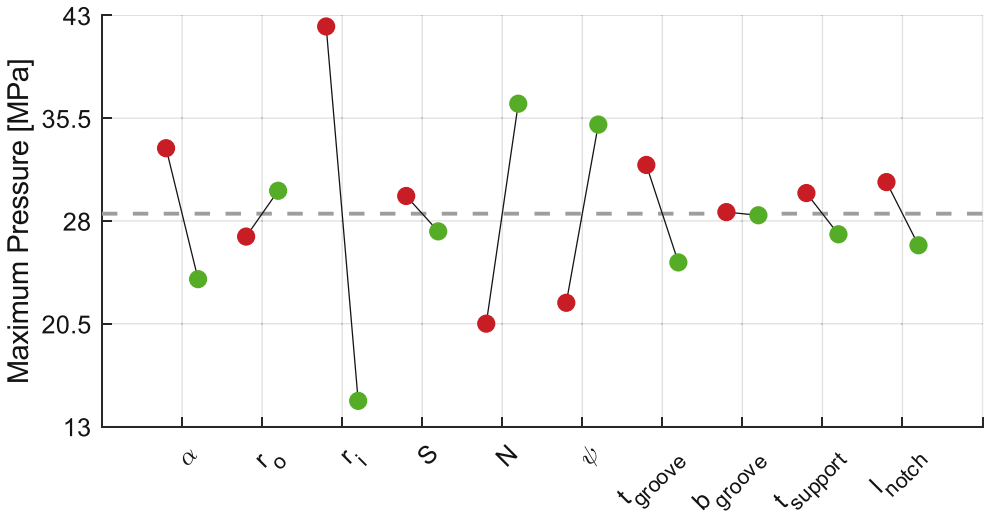

Fig. 3 Effect diagram for the output value maximum pressure

damental design feature of the Z-Pad. The position of maximum pressure for the Z-Pad is therefore mostly governed by the position of the segment center. An increase in inner radius r_i moves the center to higher radii. This increases the available surface area and thus reduces maximum pressure. Maximum pressure increases with the cone angle α. The ratio between radial and axial forces supported by the bearing is governed by the cone angle α. Thus, each applied load case is paired with a potential optimal cone angle due to its load composition. Increasing pressures suggest a lower suitability of the cone angle for the given load condition. A higher number of segments naturally results in higher pressures as this also increases the number of gaps between them. The gap area is constant for both design variations. Thus, a higher pad number N leads to less available surface area for pressure build up. As with all classic radial plain bearings clearance ψ increase naturally leads to higher maximum pressure as it worsens pressure distribution as observed in [19, 23–25].

3.2 Parameter effect regarding the position of maximum pressure

The results regarding the position of maximum pressure are depicted in Fig. 4. The position is shown normalized to the segment length. A value of 0 would denote the segment center, one of positive 1 would denote the outer edge and one of negative one would denote the inner edge. Only the global parameters of the radii r_i and r_a, the cone angle α and the clearance ψ are of significant effect. The effects of the remaining parameters are comparatively small.

Greater cone angles α move the maximum pressure further to the segment center. As maximum pressures increase (see Fig. 3) while the pressured area increases (see Fig. 6) this further indicates a worsened general suitability of the increased cone angle α, as described in 3.1. The higher amount of force that needs to be borne by each segment lead to a higher bending of the segments' edges and pressure concentrates in the center. Greater outer radii r_o move the position of maximum pressure further out relative to the segment size. Greater outside radii r_o generally stretch the design and allow for more flexibility of the overall bearing. This increased relative flexibility through longer levers moves the position of maximum pressure further outward. Larger inner radii r_i move the position of maximum pressure further inward, relative to the segment size. An inner radius increase generally compresses the whole design leading to less flexibility due to shorter levers. The increased relative stiffness centers the load. Greater clearances ψ move the position of maximum pressure further inward. Through greater clearances the overall pressure distribution is worsened. The pressured zone becomes smaller and more centered around the inflexible middle of the segment, thus moving the maximum pressure to the center.

3.3 Parameter effects regarding friction loss

The results regarding friction loss are shown in Fig. 5. Here the parameters cone angle α, outer radius r_a, the number of segments *n* and the clearance ψ are of significant influence. Of greatest influence is the outer radius. Greater radii r_o and segment number N result in an increase in friction loss while an increase in clearance ψ and an increase in cone angle α result in a reduction of friction loss. The individual influence of all remaining parameters is comparatively small.

Higher radii lead to an increase in friction loss as the increased radius moves the pressure area and thus the resulting forces further outward towards greater effective radii. A similar effect should be observable for the increase of the inner radius, as greater inner radii move the whole segment further outward. However, this effect is countered by the displacement effect the inner radius has on the pressure center (see Fig. 4). Thus, the effect of the inner radius

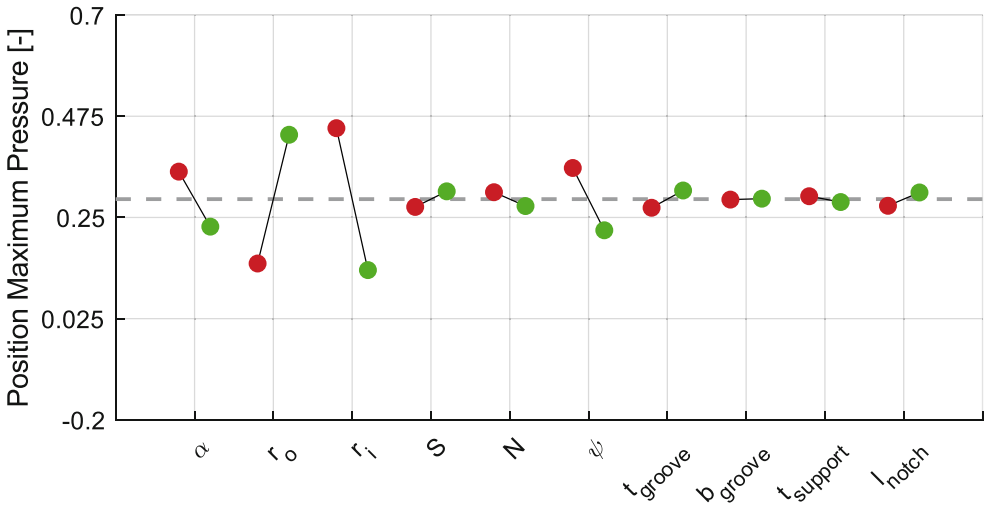

Fig. 4 Effect diagram for the output value of position of maximum pressure

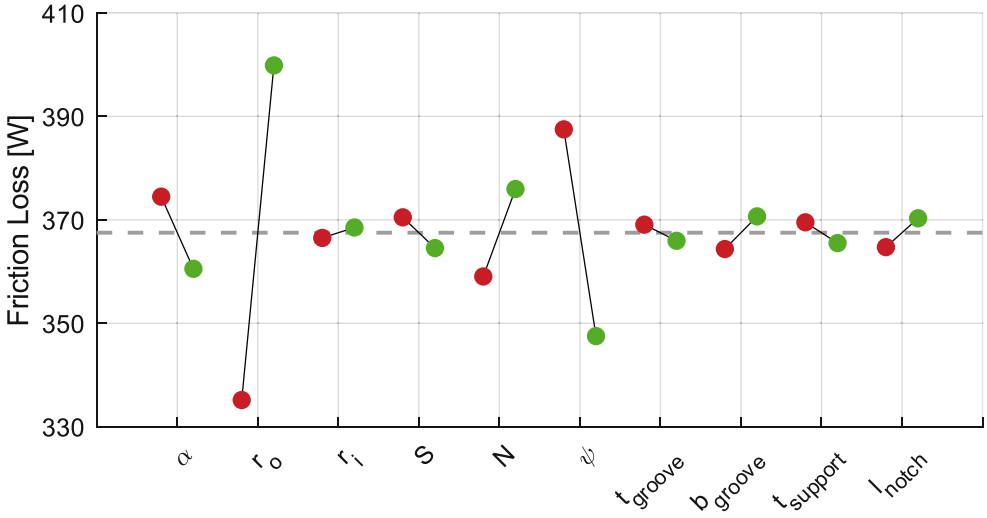

Fig. 5 Effect diagram for the output value friction loss

is comparatively small. Friction loss decreases for larger clearances. This matches the movement of the position of maximum pressure. Larger clearances worsen the pressure distribution and center the load at smaller effective radii.

3.4 Parameter effects regarding the amount of area under pressure

The parameter effects on the percentage of pressured area are depicted in Fig. 6. All effects are dominated by the bearing clearance. The cone angle α, the outer radius r_o and inner radius r_i, the span width S, the number of segments N and the length of the notch l_{notch} are of medium or small impact. The remaining parameters have no significant impact.

With increasing clearance, the pressured area decreases. This behavior is common for plain bearings and was already documented for conical plain bearings, where this correlation is especially pronounced due to the cone shape [19]. Increasing cone angles increase the pressured area, most likely due the respective angle being less suitable for the given load conditions. Increasing the outer radius reduces the percentage of loaded area. This is caused by the bearings flexibility which allows for the upper part of the segment to bend away under pressure. Naturally an outer radius increase without further adaptation of its stiffness allows for further bending and thus reduces the percentage of loaded area. The same effect can be observed for the inner radius were the correlation is inverted. A higher number of segments leads to a decrease of the pressured area as each segment features chamfers to prevent edgewear and is separated by a gap to its neighbor. With more segments, more chamfers and gaps are introduced which do not allow for pressure build-up, thus decreasing the percentage of pressured area. Lastly the pressured area increases with the length of the notch. The increased flexibility allows for a more even pressure distribution.

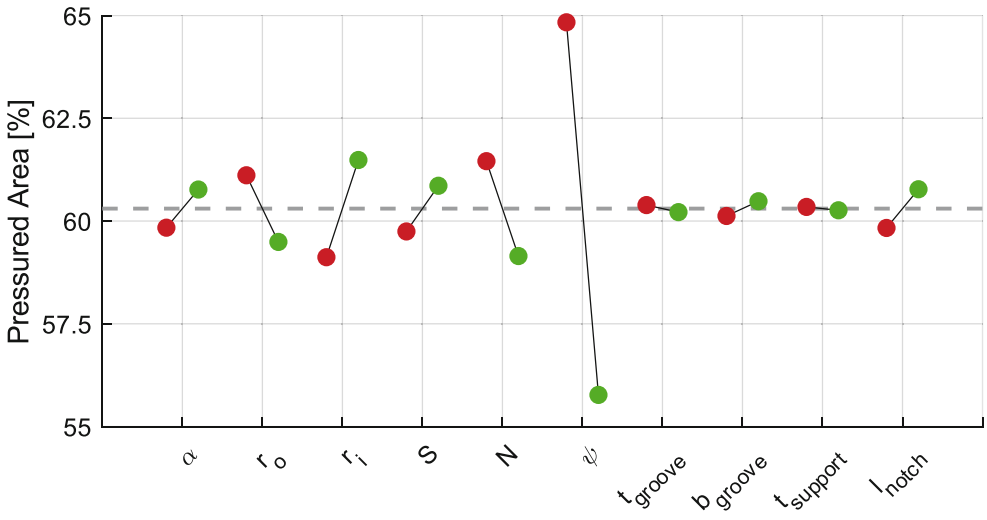

Fig. 6 Effect diagram for the output value pressured area

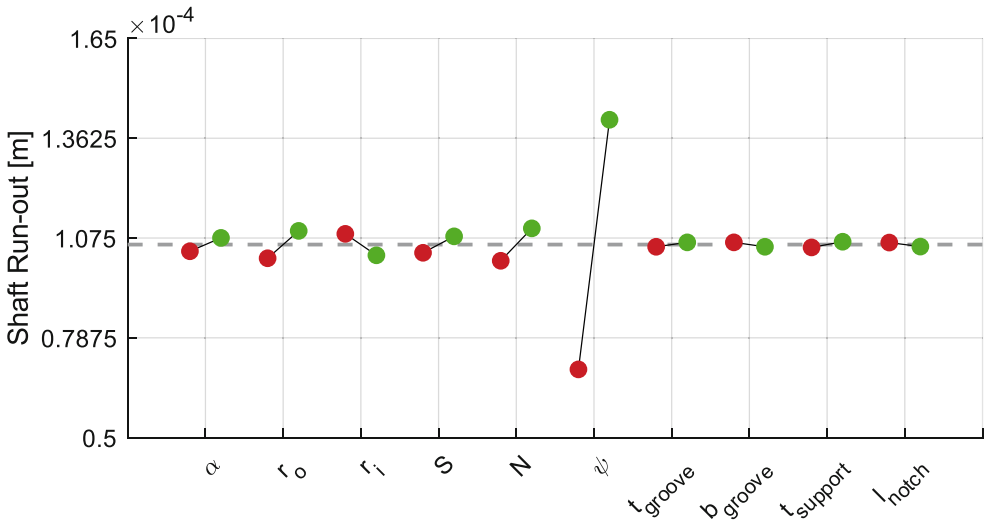

Fig. 7 Effect diagram for the output value main shaft run-out

3.5 Parameter effects regarding main shaft run-out

As expected, all parameters except the clearance are of little effect to the main shaft run-out (see Fig. 7). Shaft run-out is heavily dependent on the installed clearance as the shaft can freely move within the bounds of the clearance and is only restricted by the lubrication film height [19]. The observed run-out is still improved relative to similar FlexPad designs [12].

3.6 Discussion

In this study the effect of the available design parameters for the novel Z-Pad design on its key output values was investigated. The design parameters can be roughly grouped into two categories. The cone angle, outer and inner radius, span width, number of segments and the bearing clearance are global parameters which could also apply to a common plain bearing. The parameters of groove depth, groove width, support length and notch depth are very specific to the Z-Pad design and govern the flexible behavior of the individual segments. The investigation showed, that the influence of the global parameters is dominant in the overall bearing design. Every global design parameter but the span width S shows significant effect on at least one output value. The greatest relative effect was achieved for the inner radius r_i regarding maximum pressure. The great numerical discrepancy between the different designs is a result of the available design space. Four designs with the lower bound for inner radius showed solid body contact in the amount of 0.05 to 1.0% of the sum of all forces. These designs are not suitable.

The effect of the Z-Pad specific parameters is small for each output value. Only the notch length l_{notch} demonstrated significant influence. This behavior was to be expected as the design is overall far stiffer then the FlexPad. Therefore, the bearing's behavior is governed to a further extend by the global parameters, then the FlexPad was for the investigated design space. The influence of these parameters regarding flexibility could therefore necessitate an approach in which their influence would not be overshadowed by the global parameters. Furthermore, future studies should investigate the influence of the global parameters on the flexibility. The current bearing design allows for indirect influence of these global parameters. The outer notch was not individually parameterized and is indirectly set by the outer radius. Thus, blurring the effects of theses parameters. The groove depth is significant in its lack of influence on the bearing's performance. A design without the groove and the appendix above is therefore investigated in the following chapter.

4 Design improvement

The parameter variation of the groove width b_{groove} was without significant effect. The groove and the appendix above it (see marked area Fig. 8, left) were therefore removed and a new improved design proposed. As basis for the design parameters the parameter set P11 was chosen, as it demonstrated the best results for the target values. The improved design is shown in Fig. 8.

For this new design MB-EHD simulations with the previously investigated load condition are performed. The results are shown in Table 3.

As can be seen the results for the improved design differ only marginally from the base design of P11, while the weight is reduced by 19%.

Table 3 Simulation results for the improved design compared to P11

	Maximum Pressure [MPa]	Friction Loss [W]	Main Shaft Run-out [mm]	Segment Weight [kg]
P11	9.88	429	0.006	4.96
Improved Design	9.92	428	0.006	4.09

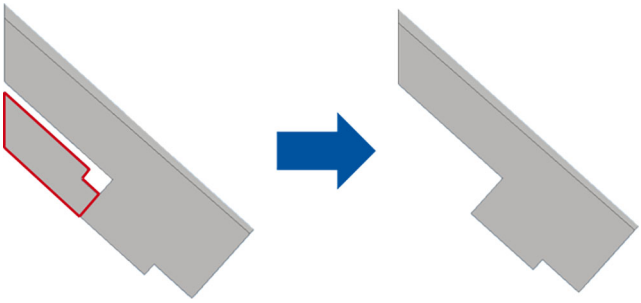

Fig. 8 Design improvement based on parameter influence, removed appendix highlighted in red

5 Conclusion

Hydrodynamic plain bearings as rotor main bearings may offer the potential to increase reliability and most importantly serviceability for wind turbines. To this end the novel Z-Pad concept was developed. In the presented study the influence of various design parameters on the performance of the novel Z-Pad plain bearing under production loads was investigated. The overall goal was a deep understanding of the relevant design choices when designing the novel plain bearing concept and to further compare the design to the previously established FlexPad, for which a similar investigation was performed [12].

The Z-Pad shows a strong relationship of its performance with the global design parameter of the radii, cone angle and clearance. Pressure position and amount strongly correspond to changes in these parameters. The Z-Pad specific parameters governing its flexibility are of relatively small impact on the hydrodynamic performance. Only the inner notch length was significant for at least one output value. The Z-Pad is overall far stiffer than the previously investigated FlexPad, which results in an overall reduced run-out compared to FlexPad bearings with similar clearance. However, the stiffer design diminishes the influence of the parameters governing the flexibility relative to the global parameters. An approach of concurrent optimization of both global parameters and flexibility parameters, therefore is unsuitable for the Z-Pad. A design process different to the one developed for the FlexPad will be necessary.

Lastly the insights from the sensitivity analysis were used to further simplify and improve the Z-Pad design. This was done by removing an appendage on the outer edge between the sliding segment and the shaft. The improved design demonstrated similar performance to the original design for the given load scenario while being reduced in weight by 19%.

Funding Open Access funding enabled and organized by Projekt DEAL.

Open Access Dieser Artikel wird unter der Creative Commons Namensnennung 4.0 International Lizenz veröffentlicht, welche die Nutzung, Vervielfältigung, Bearbeitung, Verbreitung und Wiedergabe in jeglichem Medium und Format erlaubt, sofern Sie den/die ursprünglichen Autor(en) und die Quelle ordnungsgemäß nennen, einen Link zur Creative Commons Lizenz beifügen und angeben, ob Änderungen vorgenommen wurden. Die in diesem Artikel enthaltenen Bilder und sonstiges Drittmaterial unterliegen ebenfalls der genannten Creative Commons Lizenz, sofern sich aus der Abbildungslegende nichts anderes ergibt. Sofern das betreffende Material nicht unter der genannten Creative Commons Lizenz steht und die betreffende Handlung nicht nach gesetzlichen Vorschriften erlaubt ist, ist für die oben aufgeführten Weiterverwendungen des Materials die Einwilligung des jeweiligen Rechteinhabers einzuholen. Weitere Details zur Lizenz entnehmen Sie bitte der Lizenzinformation auf http://creativecommons.org/licenses/by/4.0/deed.de.

References

1. *Communication from the comission to the european parliament, The eurpopean council, The european economic and social committee and the committee of the regions* (2022-05-18)
2. German Bundestag (2023) Gesetz für den Ausbau erneuerbarer Energien (Erneuerbare Energien-Gesetz – EEG 2023) (in Kraft getr. am 26.07.2023)
3. Energy-Charts Kreisdiagramme zur Stromerzeugung. https://energy-charts.info/charts/energy_pie/chart.htm?l=de&c=DE&year=2022&interval=year&source=total. Accessed 2023-07-24
4. Shuangwen S (2013) Report on Wind Turbine Subsystem Reliability—A Survey of Various Databases (Presentation). NREL (National Renewable Energy Laboratory)
5. Steffen B, Beuse M, Tautorat P, Schmidt TS (2020) Experience curves for operations and maintenance costs of renewable energy technologies. Joule 4(2):359–375
6. Stehly T, Duffy P (2021) cost of wind energy review
7. Stehly T, Beiter P, Duffy P (2019) Cost of Wind Energy Review
8. Hart E, Turnbull A, Feuchtwang J, McMillan D, Golysheva E, Elliott R (2019) Wind turbine main-bearing loading and wind field characteristics. Wind Energy 22(11):1534–1547
9. Abschlussbericht: *FlexPad—Entwicklung einer Auslegungsmethodik für ein innovatives Lagerungskonzept, eng.:"Final Report CWD, FlexPad"* : *Grant no.: 03EE2002B*. 2023
10. Jakobs T, Jacobs G, Rolink A, Euler J, Hollas C, Röder J (2024) Designing large segmented flexible conical plain bearings as wind turbine main bearings. J Phys: Conf Ser 2745(1):12022
11. Schröder T, Jacobs G, Rolink A, Bosse D (2019) "FlexPad"—Innovative conical sliding bearing for the main shaft of wind turbines. J Phys: Conf Ser 1222(1):12026

12. Euler J, Jacobs G, Zweiffel U, Jakobs T, Decker T, Röder J (2024) Feasibility analysis of a novel conical plain bearing with rotating segments as wind turbine main bearing. J Phys: Conf Ser 2767(5):52025
13. Abschlussbericht: *Gleitgelagertes Hauptlager einer 6 MW-Offshore-Windenergieanlage, eng.:" Final Report, HydroLa"* : *Förderkennzeichen: 0325769A*. 2020
14. Euler J, Jacobs G, Loriemi A, Jakobs T, Rolink A, Röder J (2023) Scaling challenges for conical plain bearings as wind turbine main bearings. Wind 3(4):485–495
15. Schröder TN (2021) Konisches Gleitlager für die Rotorlagerung einer Windenergieanlage, eng: "Conical Sliding Bearing for the Rotor Main Bearing of a Wind Turbine"
16. Rolink A, Jacobs G, Schröder T, Keller D, Jakobs T, Bosse D, Lang J, Knoll G (2021) Methodology for the systematic design of conical plain bearings for use as main bearings in wind turbines. Forsch Ingenieurwes 85(2):629–637
17. Plackett RL, Burman JP (1946) The design of optimum multifactorial experiments. Biometrika 33(4):305–325 (https://academic.oup.com/biomet/article/33/4/305/225377)
18. Lang, Jochen: *Schlussbericht Entwicklung einer Auslegungsmethodik für ein innovatives Lagerungskonzept FlexPad, eng.:"Final Report IST, FlexPad"* : *Teilvorhaben Elastohydrodynamische Simulation und Optimierung eines FlexPad-Lagers, eng.:"Sub-project Elastohydrodynamic simulation and optimisation of a FlexPad bearing"; Grant no. 03EE2002C*
19. Euler J, Jacobs G, Jokobs T, Röder J (2024) Feasibility study on preloaded flexible conical plain bearings as wind turbine main bearings. Tribol Schmierungstechnik 71(1). https://doi.org/10.1088/1742-6596/2767/5/052025
20. Jakobs T, Jacobs G, Euler J, Rolink A, Röder J (2024) Impact of 3D segment profiling on friction losses of plain bearings in wind turbines main bearings. J Phys: Conf Ser 2767(5):52021
21. Rolink A, Jacobs G, Müller M, Jakobs T, Bosse D (2022) Investigation of manufacturing-related deviations of the bearing clearance on the performance of a conical plain bearing for the application as main bearing in a wind turbine. J Phys: Conf Ser 2257(1):12006
22. Rolink A, Jacobs G, Pérez A, Bosse D, Jakobs T (2022) Sensitivity analysis of geometrical design parameters on the performance of conical plain bearings for use as main bearings in wind turbines. J Phys: Conf Ser 2265(3):32010
23. Hagemann T, Huanhuan D, Radtke E, Schwarze H (2021) Operating behavior of sliding planet gear bearings for wind turbine gearbox applications—part I: basic relations. Lubricants 9(10):97
24. Kuznetsov E, Glavatskih S, Fillon M (2011) THD analysis of compliant journal bearings considering liner deformation. Tribol Int 44(12):1629–1641
25. Schilling G, Liebich R (2023) The Influence of Bearing Clearance on the Load Capacity of Gas Polymer Bearings. Appl Sci 13(7):4555

Publisher's Note Springer Nature remains neutral with regard to jurisdictional claims in published maps and institutional affiliations.